Automatic segmentation of the lungs and lobes from thoracic CT scans

E. M. van Rikxoort and B. van Ginneken

Diagnostic Image Analysis Group, Department of Radiology,
Radboud University Nijmegen Medical Centre, The Netherlands

Abstract. Lung and lobe segmentation are prerequisites for automated analysis of chest CT scans. This paper presents fully automatic methods for segmentation of the lungs and lobes from thorax CT scans. Both methods have previously been published. The lung segmentation starts by automatically identifying the trachea and main bronchi. From the trachea, the lungs are found using a region growing approach. In cases for which errors are automatically detected in the resulting lung segmentation, a multi-atlas segmentation approach is applied. The lobe segmentation is based on a multi-atlas approach and was especially designed to be robust against incomplete fissures. The methods were evaluated on 55 volumetric chest CT scans provided by the LObe and Lung Analysis 2011 (LOLA11) challenge. The scans were acquired at different sites, using several different scanners, scanning protocols, and reconstruction parameters.

1 Introduction

Multi-slice CT scanning technology has revolutionized the in vivo study of the lungs and motivates the need for pulmonary image analysis [1]. Segmentation of the lungs and lobes is a prerequisite for such image analysis in chest CT scans. Accurate lung segmentation allows for the detection and quantification of abnormalities within the lungs. Segmentation of the pulmonary lobes is important to localize parenchymal disease inside the lungs and to quantify the distribution of a parenchymal disease.

A wide variety of methods for lung segmentation in 3D chest CT scans is available (e.g. [2–7]). Most of these methods rely on the fact that for normal lung parenchyma there is a large difference in attenuation between the lung parenchyma and the surrounding tissue (e.g. [2–4]). The advantages of such methods are that they are generally fast and perform well on scans that do not contain dense abnormalities. However, in the case of dense pulmonary or subpleural abnormalities, these areas are not included in the lung segmentation of these algorithms. Therefore, several methods have been developed to be able to handle pathological abnormalities, but these are often specialized for one type of abnormality. In this work, the lung segmentation as presented in [8] is applied. This method uses a hybrid approach: First, a fast, conventional lung segmentation method is applied. The result of this method are automatically

checked for possible errors based on shape measurements. To scans with failures a multi-atlas based algorithm using non-rigid registration is applied.

The pulmonary lobes are physically separated by the pulmonary fissures. When the pulmonary fissures are complete, a segmentation of the fissures equals a segmentation of the lobes. However, the pulmonary fissures are often incomplete or barely visible on chest CT scans, in which case the position of the lobar border is inferred from the airway and vessel trees and general knowledge about the shapes of lobes. Several methods for segmentation of the lobes have been published [9–14]. In this paper, we apply the method proposed in [15]. This is a fully automatic lobe segmentation method that employs the fissures, the lungs, the bronchial tree, and shape information to define the lobe borders in a multi-atlas based setup. The method was especially designed to be robust against incomplete fissures.

Results of the lung and lobe segmentation methods are presented on the 55 scans provided by the LObe and Lung Analysis 2011 (LOLA11) challenge, which contains scans acquired at different sites, using several different scanners, scanning protocols, and reconstruction parameters. Most scans contain pathologic abnormalities, ranging from mild to severe.

2 Methods

The lung and lobe segmentation methods applied have both been previously published [8, 15]. Therefore, only a short description of the methods is provided here, for details we refer to the respective original papers.

2.1 Lung segmentation

The lung segmentation applied consists of three steps. As a first step, the lungs are automatically segmented using a conventional method employing region growing and morphological smoothing. Next, automatic error detection is applied. The scans that are likely to contain errors are then segmented by a multi-atlas segmentation.

Conventional lung segmentation The conventional lung segmentation consists of four steps: (1) Extraction of the large airways; (2) Segmentation of the lung regions; (3) Separation of the left and right lungs; (4) Smoothing. Each step is shortly described below.

1. The trachea and main bronchi are found using region growing. The seed point for the region growing is automatically determined by searching for a round, connected region on axial slices with an average Hounsfield Unit (HU) below -950. Using the voxel with the lowest HU within the found region as a seed, the trachea and main stem bronchi are grown using explosion controlled region growing. From the result, the point with the lowest HU is taken as seed point for the next step.

2. The lungs are segmented using region growing from the new seed point. Optimal thresholding as described by Hu et al. [3] is used to determine the upper threshold for this region growing operation.
3. After the lungs are grown, the trachea and bronchi found in the first step are removed from the results to obtain only the lungs. In cases where only one connected component is found for the lungs, the lungs are separated by applying dynamic programming in axial slices.
4. As a final step for the lung segmentation, each lung is smoothed separately using 3D hole filling and morphological closing with a spherical structuring element of size 11 to include vessels in the segmentation and smooth the borders.

Error Detection The segmentation results of the conventional lung segmentation are automatically checked for errors to identify scans for which multi-atlas segmentation should be applied. For this paper, only shape analysis was applied for the error detection. The shape analysis checks if the shape of the costal lung surface is convex by comparing to the convex hull of the lungs. If the difference between the convex hull and the segmented lung in the costal lung surface is large, it is likely that an error occurred.

Multi-atlas lung segmentation The multi-atlas segmentation applied follows the general scheme of multi-atlas segmentation with averaging as a decision fusion; A set of eight atlases is registered to the test image and the labels are propagated. For each voxel in the test image, the propagated labels are averaged and the result is subsequently thresholded at 0.5. For a description of the atlases used see [8].

2.2 Lobe segmentation

The lobe segmentation is based on a multi-atlas scheme in which information from scans with complete fissures is transformed to the test scan. In the case of lobe segmentation, the goal of the registration is to transform the atlas to the test scan in such a way that the lobar borders line up. Directly registering chest CT scans from different subjects does not lead to satisfactory results due to anatomical variations inside the lungs; the fissures do generally not line up after registration. Therefore, instead of registering the original chest CT data, the atlas is constructed by combining automatically extracted anatomical segmentations of the lungs, fissures, and airways.

3 Experiment and Results

The methods were applied to all 55 scans of the LOLA11 segmentation challenge. The conventional lung segmentation took on average 20 seconds per scan on a single core PC. For 14 scans, the multi-atlas lung segmentation was applied after

the error detection indicated possible errors. For these 14 scans, the multi-atlas lung segmentation took on average 120 minutes per scan. The segmentation of the lobes took on average 110 minutes per scan on a single core PC. The results were submitted to the LOLA11 website, where the evaluation was performed. Evaluation was performed in terms of overlap, where overlap between two binary volumes was defined as the volume of their intersection divided by the volume of their union. A slack border of 2mm around the reference standard was used to account for discrepancies at the lung border. Table 1 shows the results of our method for lung segmentation. It can be seen that although the average overlap is high there are scans for which the method completely fails, with a minimum overlap of 0.019. In Table 2 the results for our lobe segmentation are provided. It can be appreciated that the results for the right middle lobe are substantially worse than for the other lobes. Figures 1, 2, 3, 4 show examples of lung and lobe segmentations of our methods on four different scans from LOLA11.

Table 1. Results of lung segmentation for the 55 scans in LOLA11.

	mean	SD	min	Q1	median	Q3	max
left lung	0.964	0.11	0.283	0.982	0.991	0.995	0.997
right lung	0.959	0.162	0.019	0.989	0.994	0.996	0.999
score	0.962						

Table 2. Results of lobe segmentation for the 55 scans in LOLA11.

	mean	SD	min	Q1	median	Q3	max
left upper lobe	0.930	0.133	0.359	0.944	0.977	0.989	0.995
left lower lobe	0.895	0.204	0.037	0.933	0.975	0.983	0.995
right upper lobe	0.870	0.181	0.000	0.834	0.950	0.977	0.998
right middle lobe	0.647	0.345	0.000	0.410	0.850	0.918	0.987
right lower lobe	0.913	0.134	0.311	0.912	0.965	0.980	0.995
score	0.851						

4 Discussion & Conclusion

In this paper, previously proposed methods for segmentation of the lungs and lobes [8, 15] were applied to the data from the LOLA11 challenge without changes of the methods or parameters. The results show that the methods perform well on average but there are several scans for which the methods fail. After visually checking the results, we conclude that the main reasons for the failures in the lung segmentation are that the method is not able to include some severe abnormalities at the lung border. Although the multi-atlas based segmentation

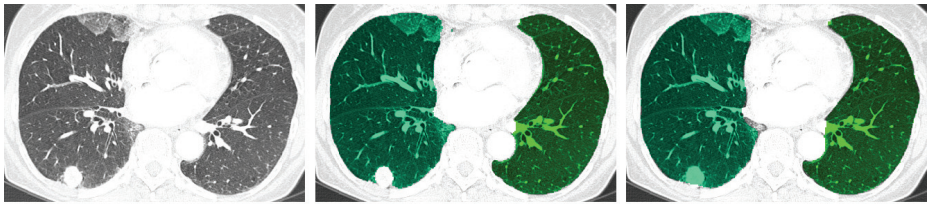

Fig. 1. Example of the lung segmentation results for case lola11-10. The left frame shows the original slice, in the middle the result of the conventional lung segmentation is shown. An error was detected in the right lung after which the multi atlas method was applied. The results of the multi-atlas method are shown in the right frame. The dense abnormality is now included in the lung segmentation but at the borders the multi-atlas segmentation is less precise than the conventional method.

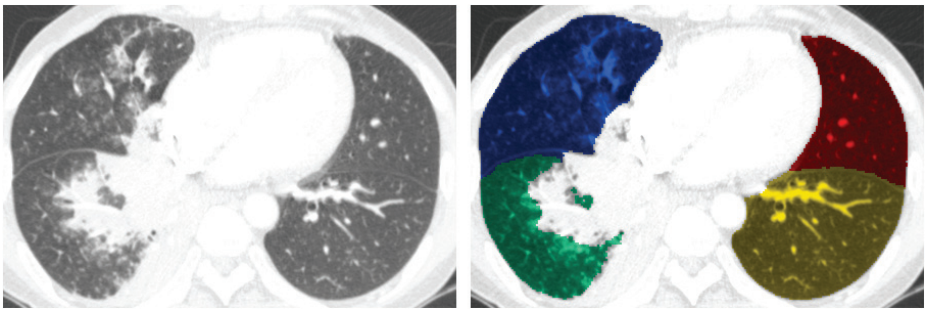

Fig. 2. Example output of the lung and lobe segmentation for case lola11-02. The right lung contains pathologic abnormalities which were not included in our lung segmentation. Since the error checking in the hybrid lung segmentation method was set to only check the shape of the costal lung surface, this scan was segmented using the conventional lung segmentation method. The segmentation of the lobes seems not to be affected by the error in the lung segmentation.

performs slightly better in this aspect than the conventional method, it still often doesn't find the lung borders correctly. For the segmentation of the lobes, the main problems arise either from abnormalities around the fissures leading to failures of the fissure detection or severely altered lobar shapes that can not be handled by the registration.

As shown in Figure 1, the hybrid lung segmentation is sometimes able to correct the errors in the conventional lung segmentation, but on the other hand is less precise at the borders of the lungs. As a result, the overall performance of the lung segmentation method does not improve much with the hybrid approach compared to the conventional approach for lung segmentation. A possible solution would be to only use the results of the multi-atlas segmentation locally at the locations where errors were detected.

Since overall overlap measures were computed for evaluation, the errors in the lung segmentation are also reflected in the quantitative results of the lobar

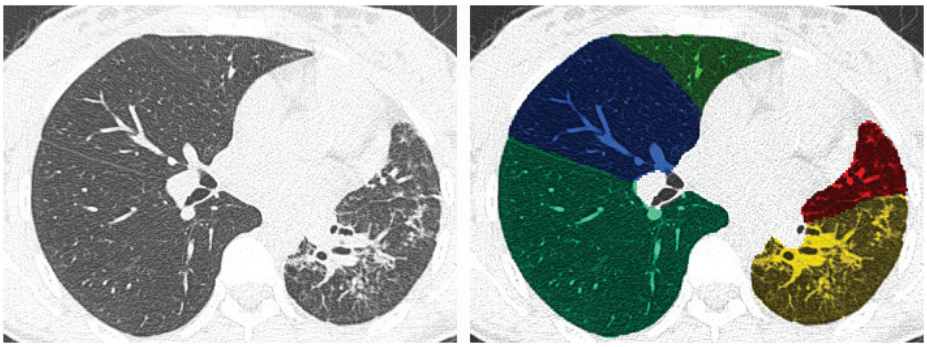

Fig. 3. Example output of the lung and lobe segmentation for case lola11-04. Despite pathologic abnormalities in the left lung, the lung and lobe segmentations are still able to generate a good result.

segmentation. For some cases, e.g. the case shown in Figure 2 the lung segmentation is incorrect but the lobar boundary was correctly identified. The lobe segmentation mainly failed in cases that showed a lot of pathologic abnormalities, leading to failures of the input segmentations of lungs, fissures, and airways. We believe that for some of the cases in the LOLA11 set, which are very abnormal, an interactive approach, such as for example proposed in [14], would be the best solution since it is unlikely that automatic methods will be able to solve these kind of cases.

The atlas-registration applied for the lobe segmentation is designed to produce a valid lobe shape in cases with incomplete fissures. For this reason, the atlas-registration is designed in such a way that it is notable to deform much from the shapes in the atlases. For cases in which severe abnormalities alter the shapes of the lobes, which is the case for some scans in LOLA11, the applied registration is not able to deform to these shapes. We observed that in these kind of cases, the fissures are often found correctly but the following atlas registration is not able to align the fissures in the atlas and the test scan. As a result, the lobar segmentation is incorrect. We will investigate for future work how we can solve this problem. Since fissure detection also sometimes leads to spurious responses simple forcing the atlas to always follow the found fissures does not produce adequate results.

In conclusion, we have presented the application of fully automatic lung and lobe segmentation methods to the set of 55 scans of the LOLA11 challenge. The results show that the methods are on average successful in segmenting the lungs and lobes, but in cases with severe abnormalities the methods fail.

References

1. Sluimer, I., Schilham, A., Prokop, M., van Ginneken, B.: Computer analysis of computed tomography scans of the lung: A survey. IEEE Transactions on Medical Imaging **25**(4) (2006) 385–405

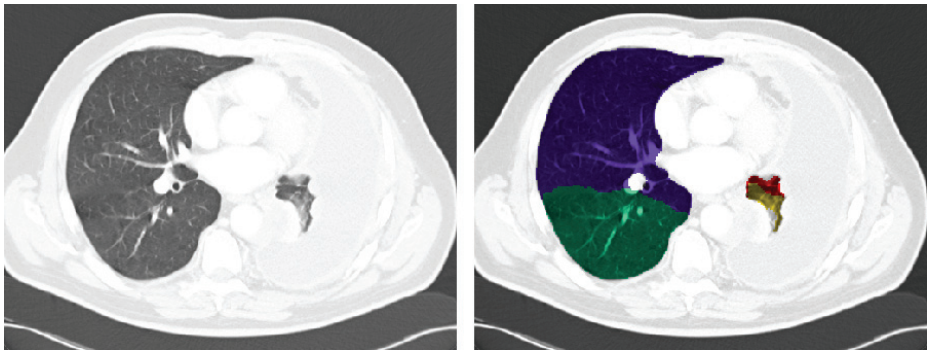

Fig. 4. Example output of the lung and lobe segmentation for case lola11-45. This case has a larger slice thickness than most scans (1.5mm) which does not affect our lung segmentation but does harm the detection of the pulmonary fissures for the lobe segmentation. The left lung seems to have collapsed, which leads to our lung segmentation only segmenting the aerated areas. The lobe segmentation always produces a result but for such cases the result is not correct.

2. Armato, S.G., Sensakovic, W.F.: Automated lung segmentation for thoracic CT: Impact on computer-aided diagnosis. Academic Radiology **11**(9) (2004) 1011–1021
3. Hu, S., Hoffman, E., Reinhardt, J.: Automatic lung segmentation for accurate quantitation of volumetric X-ray CT images. IEEE Transactions on Medical Imaging **20**(6) (2001) 490–498
4. Brown, M.S., McNitt-Gray, M.F., Mankovich, N.J., Goldin, J.G., Hiller, J., Wilson, L.S., Aberle, D.R.: Method for segmenting chest CT image data using an anatomical model: Preliminary results. IEEE Transactions on Medical Imaging **16**(6) (1997) 828–839
5. Pu, J., Roos, J., Yi, C.A., Napel, S., Rubin, G.D., Paik, D.S.: Adaptive border marching algorithm: Automatic lung segmentation on chest CT images. Computerized Medical Imaging and Graphic **32**(6) (2008) 452–462
6. Prasad, M.N., Brown, M.S., Ahmad, S., Abtin, F., Allen, J., da Costa, I., Kim, H.J., McNitt-Gray, M.F., Goldin, J.G.: Automatic segmentation of lung parenchyma in the presence of diseases based on curvature of ribs. Academic Radiology **15**(9) (2008) 1173–1180
7. Sluimer, I., Prokop, M., van Ginneken, B.: Towards automated segmentation of the pathological lung in CT. IEEE Transactions on Medical Imaging **24**(8) (2005) 1025–1038
8. van Rikxoort, E.M., de Hoop, B., Viergever, M.A., Prokop, M., van Ginneken, B.: Automatic lung segmentation from thoracic computed tomography scans using a hybrid approach with error detection. Medical Physics **36**(7) (2009) 2934–2947
9. Kuhnigk, J.M., Dicken, V., Zidowitz, S., Bornemann, L., Kuemmerlen, B., Krass, S., Peitgen, H.O., Yuval, S., Jend, H.H., Rau, W.S., Achenbach, T.: New tools for computer assistance in thoracic CT part 1. Functional analysis of lungs, lung lobes and bronchopulmonary segments. Radiographics **25** (2005) 525–536
10. Zhang, L., Hoffman, E.A., Reinhardt, J.M.: Atlas-driven lung lobe segmentation in volumetric x-ray CT images. IEEE Transactions on Medical Imaging **25**(1) (2006) 1–16

11. Pu, J., Zheng, B., Leader, J.K., Fuhrman, C., Knollmann, F., Klym, A., Gur, D.: Pulmonary lobe segmentation in ct examinations using implicit surface fitting. IEEE Transactions on Medical Imaging **28**(12) (2009) 1986–1996
12. Ukil, S., Reinhardt, J.M.: Anatomy-guided lung lobe segmentation in X-ray CT images. IEEE Transactions on Medical Imaging **28**(2) (2009) 202–214
13. van Rikxoort, E.M., de Hoop, B., van de Vorst, S., Prokop, M., van Ginneken, B.: Automatic segmentation of pulmonary segments from volumetric chest CT scans. IEEE Transactions on Medical Imaging **28**(4) (2009) 621–630
14. Lassen, B., Kuhnigk, J.M., van Rikxoort, E.M., Peitgen, H.O.: Interactive lung lobe segmentation and correction in tomographic images. In: Medical Imaging. Volume 7963 of Proceedings of the SPIE. (2011) 79631S–1–79631S–6
15. van Rikxoort, E.M., Prokop, M., de Hoop, B., Viergever, M., Pluim, J., van Ginneken, B.: Automatic Segmentation of Pulmonary Lobes Robust Against Incomplete Fissures. IEEE Transactions on Medical Imaging **29**(6) (2010) 1286–1296